

# PROPOSAL FOR EXPERIMENT AT LEPS BEAM LINE

July 14, 2001

## Photoproduction of $2\pi^0$ with Nuclear Targets

### SPOKESPERSON:

SHIMIZU Hajime  
Department of Physics, Yamagata University  
Yamagata 990-8560  
e-mail: hshimizu@sci.kj.yamagata-u.ac.jp  
phone: 023-628-4762  
FAX: 023-628-4567

### EXPERIMENTAL GROUPS:

H. Shimizu, Y. Tajima, and H.Y. Yoshida  
*Department of Physics, Yamagata University*  
J. Kasagi, T. Kinoshita, T. Nakabayashi, and H. Yamazaki  
*Laboratory of Nuclear Science, Tohoku University*  
T. Matsumura and T. Yorita  
*Research Center for Nuclear Physics, Osaka University*  
P. Shagin  
*Institute for High Energy Physics, Protvino, Russia*

### RUNNING TIME:

- 2 days for tuning and calibration
- 30 days for data acquisition

### BEAM:

- Type of Polarization: Linearly polarized LEPS beam
- Beam Intensity:  $\geq 2 \times 10^6$  photons/s  
( $\geq 8 \times 10^5$  photons/s for  $E_\gamma \geq 1.5$  GeV)

### DETECTOR:

Backward  $\gamma$ -detector (252 Pb/SCIFI blocks) +  $\alpha$

### TARGETS:

- 3 nuclear targets,  $C, Cu, W$
- A solid Hydrogen target (5cm thick)

# Summary of the Proposal

We propose an experiment for  $2\pi^0$  photoproduction in nuclei, utilizing multi-GeV Laser-Electron Photons at SPring-8 (LEPS). The main purpose of the proposed experiment is to search for a precursory phenomenon to the chiral transition. For this purpose we measure the process  $\gamma A \rightarrow \pi^0\pi^0 pX$  by detecting  $4\gamma$ 's and a proton to see whether an enhancement appears or not in the  $\pi^0\pi^0$  mass spectrum reflecting the  $\sigma$  meson near the  $2\pi$  threshold at a high momentum-transfer region.

The main detector is a backward  $\gamma$ -detector covering the solid angle of about  $2\pi$  sr, consisting of 252 lead/scintillating fiber (Pb/SCIFI) blocks which have been completed and mounted. The whole  $\gamma$ -detector system has been tested with the LEPS beam. And we have confirmed that it works well. We are planning to install a circular disk of plastic scintillators at a forward angular region to identify the proton. Photon-veto counters of lead glass will be placed just after the circular disk. Other photon-veto counters are also installed just in front of the target to reduce the background originated by the beam halo as well as to veto the  $\gamma$ 's going out of the uncovered region of the  $\gamma$  detector.

We employ three conventional targets,  $C$ ,  $Cu$ , and  $W$ . In addition to that we are planning to use a solid Hydrogen target with which the data in free space will be obtained and compared to the data with the nuclear targets. We will start the experiment without the solid Hydrogen target at first. But the data only with the nuclear targets are thought to be still meaningful by comparing the data for different momentum-transfer regions. Comparison of the data will be made as well for different momenta of the  $\sigma$  in the nucleus. This will be the first measurement of the  $\pi^0\pi^0$  mass spectrum with nuclear targets at the energy of multi-GeV.

We also try to find a clue to partial restoration of chiral symmetry in the asymmetry parameter  $\Sigma(\theta)$  in the  $\gamma A \rightarrow \pi^0\pi^0 pX$  process. The asymmetry parameter is measured with a linearly polarized photon beam. This will also be the first measurement of the polarization observable  $\Sigma(\theta)$  for photoproduction of  $\pi^0\pi^0$  with nuclear targets in the energy region of multi-GeV.

# Contents

<b>1</b>	<b>Physics Motivation</b>	<b>4</b>
1.1	<i>Chiral Symmetry in QCD</i> . . . . .	4
1.2	<i>Precursors to Chiral Transition in Nuclei</i> . . . . .	4
<b>2</b>	<b>Proposed Experiment at LEPS</b>	<b>7</b>
2.1	<i>General Description of the Experiment</i> . . . . .	7
2.2	<i>Experiment with Photon Beam</i> . . . . .	8
2.3	<i><math>\gamma</math> Detector</i> . . . . .	8
2.3.1	Energy Calibration . . . . .	10
2.3.2	Clustering Algorithm . . . . .	11
2.4	<i>Results of the Test Experiment</i> . . . . .	12
2.5	<i>Data Statistics</i> . . . . .	16
2.5.1	Expected Yield . . . . .	17
2.5.2	Target Empty Run . . . . .	18
<b>3</b>	<b>Conclusion and Requests</b>	<b>19</b>

# 1 Physics Motivation

## 1.1 *Chiral Symmetry in QCD*

It is widely accepted that chiral symmetry is one of the most fundamental properties of QCD and is spontaneously broken in our real world. The chiral symmetry is, consequently, not apparent in the hadron spectrum. Actually, scalar and pseudoscalar mesons are not degenerate in mass, for example. Nevertheless the chiral symmetry plays a crucial role in hadron physics. The most prominent success is that the existence of the pions with very small mass is explained by the breakdown of this chiral symmetry. In this scenario the pseudoscalar pions are Goldstone bosons of chiral symmetry breaking and the scalar  $\sigma$  is regarded as the Higgs boson of the strong interaction. Thus the  $\sigma$  meson is a fundamental feature of the QCD vacuum.

It is important in the study of QCD to realize chiral symmetry restoration experimentally as much as we can. There are some projects going on to search for experimental manifestations of Quark-Gluon Plasma in which chiral symmetry is restored via the chiral transition. It might be difficult, however, to handle the data without the knowledge of hadron characteristics in the transient region of the phase transition. It is therefore quite important to reveal how the chiral transition takes place and what kind of precursory phenomena come about. A signal of partial restoration of chiral symmetry would give a clue to the essential understanding of the QCD vacuum and hence of hadron physics.

## 1.2 *Precursors to Chiral Transition in Nuclei*

The inside of the nucleus is one of the candidates where precursors to the chiral transition might appear due to partial restoration of chiral symmetry in dense matter. We try to find precursory phenomena to the chiral transition in nuclei in our experiment proposed here. The pions and the  $\sigma$  are understood as the fluctuations of the phase and the amplitude of the chiral order parameter  $\langle \bar{q}q \rangle$ , respectively. Therefore a bigger change of the characteristics of the  $\sigma$  meson would be expected than that of other hadrons since the  $\sigma$  is closely related to the order parameter. Actually it is pointed out that partial restoration of chiral symmetry may take place even at the normal nuclear density,  $\rho_0 = 0.17 fm^{-3}$ , and then the  $\sigma$  may show up as a sharp resonance in nuclei[1] although it appears only as a broad resonance in free space.

For simplicity, we consider the  $\sigma$  at rest in the nuclear medium. Then the propagator  $D_\sigma$  is written by

$$D_\sigma^{-1}(\omega) = \omega^2 - m_\sigma^2 - \Sigma_\sigma(\omega; \rho) \quad (1)$$

where  $m_\sigma$  is the mass of the  $\sigma$  in the tree level and  $\Sigma_\sigma(\omega; \rho)$  shows the loop corrections in the vacuum as well as in the medium. The spectral function  $S_\sigma(\omega)$  is then defined as

$$S_\sigma(\omega) = -\frac{1}{\pi} \text{Im} D_\sigma(\omega) \quad (2)$$

$$= -\frac{1}{\pi} \frac{\text{Im} \Sigma_\sigma}{(\omega^2 - m_\sigma^2 - \text{Re} \Sigma_\sigma)^2 + (\text{Im} \Sigma_\sigma)^2}. \quad (3)$$

The effective mass  $m_\sigma^*$  of the  $\sigma$  is defined by

$$\text{Re} D_\sigma^{-1}(\omega = m_\sigma^*) = [\omega^2 - m_\sigma^2 - \text{Re} \Sigma_\sigma]_{\omega=m_\sigma^*} = 0. \quad (4)$$

On the other hand,  $m_\sigma^*$  and  $m_\pi$  get degenerate when chiral symmetry is restored. Namely at the critical density, which is thought to be  $\rho \simeq (3 - 5)\rho_0$ ,  $m_\sigma^* = m_\pi$  and we have

$$\text{Re} D_\sigma^{-1}(\omega = m_\pi) = [\omega^2 - m_\sigma^2 - \text{Re} \Sigma_\sigma]_{\omega=m_\pi} = 0. \quad (5)$$

Therefore there must be a density  $\rho_c$  at which the real part of the propagator vanishes with  $\omega = 2m_\pi$ . Then we have

$$\text{Re} D_\sigma^{-1}(\omega = 2m_\pi) = [\omega^2 - m_\sigma^2 - \text{Re} \Sigma_\sigma]_{\omega=2m_\pi} = 0 \quad (6)$$

at the density  $\rho_c$ . Consequently, the spectral function is represented with the imaginary part of the propagator,

$$S_\sigma(\omega \simeq 2m_\pi) = -\frac{1}{\pi \text{Im} \Sigma_\sigma} \quad (7)$$

at that density. Here,  $\text{Im} \Sigma_\sigma$  corresponds to the width of the  $\sigma$  and therefore it is proportional to the phase space factor, then we have

$$S_\sigma(\omega \simeq 2m_\pi) \propto \frac{\theta(\omega - 2m_\pi)}{\sqrt{1 - (4m_\pi^2/\omega^2)}}. \quad (8)$$

This shows that an enhancement of the spectral function of the  $\sigma$  would come about near the  $2\pi$  threshold. An order estimation of the one-loop corrections to the self-energy of the  $\sigma$  also gives the same result.

Next thing to do is to find the value of the density  $\rho_c$  and the behavior of the spectral function near the normal nuclear density  $\rho_0$ . The chiral condensate in nuclear medium  $\langle \sigma \rangle$  at the density  $\rho$  may be parameterized as

$$\langle \sigma \rangle \equiv \sigma_0 \Phi(\rho) \quad (9)$$

and

$$\Phi(\rho) = 1 - C \frac{\rho}{\rho_0} \quad (10)$$

in the linear density approximation. The in-medium spectral function of the  $\sigma$  is calculated in the one-loop level with a simple  $SU(2)$  linear  $\sigma$  model,

$$\mathcal{L} = \frac{1}{4} tr \left[ \partial M \partial M^\dagger - \mu^2 M M^\dagger - \frac{2\lambda}{4!} (M M^\dagger)^2 - h(M + M^\dagger) \right], \quad (11)$$

where  $tr$  is for the flavor index and  $M = \sigma + i\vec{\tau} \cdot \vec{\pi}$ . The coupling constants  $\mu^2$ ,  $\lambda$ , and  $h$  have been determined so as to reproduce  $f_\pi = 93$  MeV and  $m_\pi = 140$  MeV, as well as the S-wave  $\pi - \pi$  phase shifts in the one-loop order. Employing the Lagrangian we have

$$\Phi(\rho_c) = 0.74 \quad (12)$$

in the case of  $m_\sigma^* = 550$  MeV. And with a reasonable value of  $C \simeq 0.2$ , we obtain

$$\rho_c = 1.25\rho_0, \quad (13)$$

which is not far from the normal nuclear density. We see that  $\Phi(\rho_0) = 0.8$  at the normal nuclear density. Fig. 1 shows the spectral functions of the  $\sigma$  for several values of  $\Phi$ . The

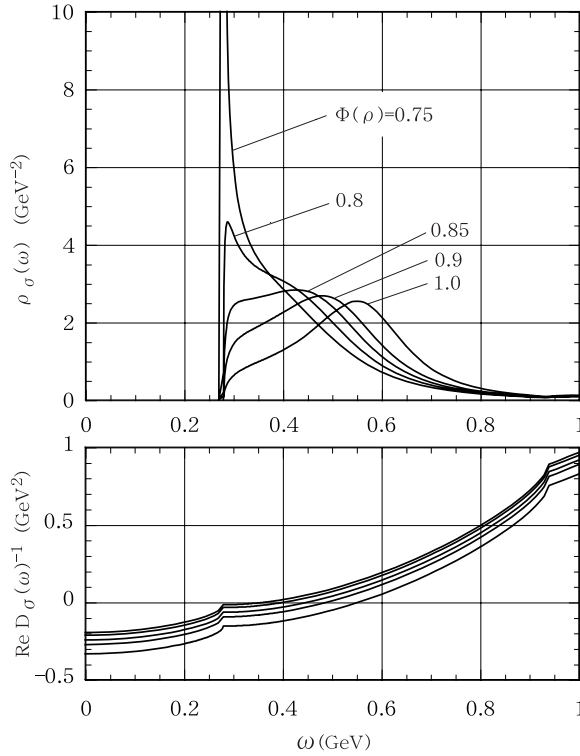


Figure 1: Spectral functions for the  $\sigma$  (upper part) and the real part of the inverse propagator (lower part) for several values of  $\Phi = \langle \sigma \rangle / \sigma_0$  with  $m_\sigma^* = 550$  MeV. In the lower panel, lines correspond to different values of  $\Phi$  decreasing from bottom to top.

characteristic enhancement is seen just above the  $2\pi$  threshold even at the normal nuclear

density. We can translate the spectral function to the  $\pi\pi$  invariant mass distribution reflecting the  $\sigma$  meson. And there is a chance to find the enhancement in the  $2\pi$  invariant mass distribution near the  $2\pi$  threshold region.

## 2 Proposed Experiment at LEPS

### 2.1 General Description of the Experiment

The main purpose of the proposed experiment is to search for a precursory phenomenon to the chiral transition. We are planning to measure  $2\pi^0$  events with nuclear targets to see whether an enhancement appears or not in the  $\pi^0\pi^0$  mass spectrum near the  $2\pi$  threshold at a high momentum-transfer region. The main decay channel of the  $\sigma$  meson is  $\sigma \rightarrow \pi\pi$ . The measurement of  $\pi^+\pi^-$  events is no good for this purpose since there are huge backgrounds coming from the  $\rho^0 \rightarrow \pi^+\pi^-$  process. This is the first measurement of the  $\pi^0\pi^0$  mass spectrum with nuclear targets at the energy region of GeV.

We measure the process  $\gamma A \rightarrow \pi^0\pi^0 pX$  by detecting  $4\gamma$ 's and a proton. The main detector is a backward  $\gamma$ -detector covering the solid angle of about  $2\pi$  sr. (A detail explanation for the  $\gamma$  detector will be given afterwards.) We install a circular disk of plastic scintillators at a forward angular region to identify the proton. Photon-veto counters of lead glass are placed just after the circular disk. Other photon-veto counters are also installed just before the target to reduce the background originated by the beam halo as well as to veto the  $\gamma$ 's going out of the uncovered region of the  $\gamma$  detector.

We employ three conventional targets which are a 4 cm thick Carbon block, a stack of 0.5 mm thick Copper plates, and that of thin Tungsten films. The net thickness of each target is adjusted to be about 0.2 radiation lengths. In addition to that we are planning to use a solid Hydrogen target with which the data in free space will be obtained and compared to the data with the nuclear targets. A solid Hydrogen target has been used successfully at LNS, Tohoku University. We will start the experiment without the solid Hydrogen target at first. But the data only with the nuclear targets are thought to be still meaningful by comparing the data for different momentum-transfer regions. Comparison of the data will be made as well for different momenta of the  $\sigma$  in the nucleus.

The asymmetry parameter  $\Sigma$  for  $2\pi^0$  photoproduction will also be measured with a linearly polarized photon beam. There are only two facilities capable of supplying a multi-GeV linearly polarized photon beam with good quality at present in the world. Those are LEPS (2.4 GeV) and GRAAL (1.5 GeV). (A new beam line for polarized photons is now under construction at Jefferson Laboratory in the US by utilizing a diamond crystal.

The peak energy of the polarized beam is 2 GeV and the beam intensity is expected to be something like  $1 \times 10^6$  photons/s.) However there have been no experiments with nuclear targets at GRAAL. Therefore this will also be the first measurement of the polarization observable  $\Sigma$  for photoproduction of  $\pi^0\pi^0$  with nuclear targets in the energy region of multi-GeV.

## 2.2 *Experiment with Photon Beam*

The photon beam is still of good advantage to produce mesons inside the nucleus effectively although it plays mostly as a vector meson beam because of vector meson dominance in the relevant energy region. In production of the  $\sigma(\pi^0\pi^0)$  there are lots of events due to peripheral production if a hadron beam, such as the proton and the pion, is utilized. On the contrary it is kind of difficult to produce scalar mesons peripherally in the case of the photon beam except at very forward angular region (the Primakov region). Therefore the photon beam is more suitable in producing the  $\sigma$  inside the nucleus compared with the case of the hadron beam.

We employ a Laser-Electron Photon beam at SPring-8 (LEPS). The LEPS beam is obtained by means of backward Compton scattering of laser photons on 8 GeV electrons in the storage ring. The maximum energy of the beam is 2.4 GeV for the time being. Unlike the photon beam produced by Bremsstrahlung of electrons, the LEPS beam is much superior in the energy distribution of the beam, namely low energy photons are not dominated in the beam. In addition to that, it is very easy to have a photon beam polarized almost 100%, which is a big advantage of the LEPS beam. (In the case of the polarized photon beam under construction at Jefferson Laboratory, the polarization are expected to be  $\sim 70\%$ .) There are neither experimental data nor predictions unfortunately for the asymmetry parameter  $\Sigma$  of  $2\pi$  photoproduction taking place in nuclear matter so far. But we have good experiences with measurements of spin observables giving a striking experimental result which nobody had foreseen before, such as the EMC effect etc. In this regard the polarization measurement might give a new aspect in the process of chiral symmetry restoration.

## 2.3 *$\gamma$ Detector*

We have constructed a backward  $\gamma$ -detector illustrated with Fig. 2. We utilize the backward  $\gamma$ -detector to detect multi- $\gamma$ 's originated from  $\pi^0$ 's. The detector covers the polar angle from  $30^\circ$  to  $100^\circ$  with full azimuthal angles, corresponding to a solid angle of about  $2\pi$  sr. At the center of the detector, there is an empty space measures 60 cm in diameter



around the target position. The backward  $\gamma$ -detector is an electromagnetic calorimeter consisting of 252 detector modules. The angular interval between two adjacent modules is  $10^\circ$  for the both directions. Each detector module comprises a lead/scintillating fiber (Pb/SCIFI) block[2], a light guide, and a photomultiplier tube. As for the Pb/SCIFI block, a matrix of 1mm diameter scintillating fibers is embedded in a lead block and parallelly aligned. Consequently the fibers are placed exactly on the corners of equilateral

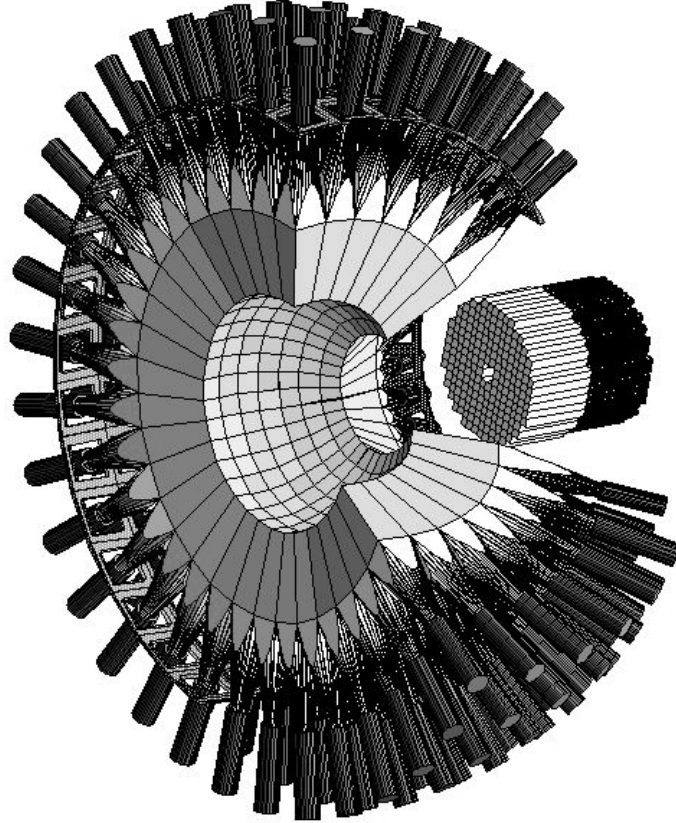


Figure 2: Schematic view of the  $\gamma$ -detector complex. The backward  $\gamma$ -detector (bigger one) consists of 252 Pb/SCIFI blocks and the forward  $\gamma$ -detector comprises 252  $\text{PbWO}_4$  crystal scintillators.

triangles with a fiber-to-fiber spacing of 1.35 mm. The volume ratio of fiber to lead to epoxy is 50:35:15. The Pb/SCIFI blocks were built at first in the full rectangular shape with fibers running along the length of each block. Then four long sides of the block were machined to the appropriate form. The shape and the length of the light guide were determined using a ray-tracing simulation.

The whole detector system is a kind of basket with a hemisphere shape, as shown in Fig. 2, having a function of rotation with respect to an axis perpendicular to the beam. At first the empty basket was rotated by  $90^\circ$  and detector modules were mounted onto the basket. This work was done at first for the layer corresponding to  $\theta = 100^\circ$ , then next

layer of  $\theta = 90^\circ$ , and so on, from bottom to up. After the mounting was completed the whole detector system was rotated back as it should be.

### 2.3.1 Energy Calibration

Prior to the calibration experiment, we tested the response of detector modules to cosmic rays. Cosmic muon peaks measured by some typical Pb/SCIFI modules were utilized to determine the optimum high voltage value of each photomultiplier tube (Fig. 3). According to a GEANT3 Monte-Carlo simulation, the average energy deposit caused by

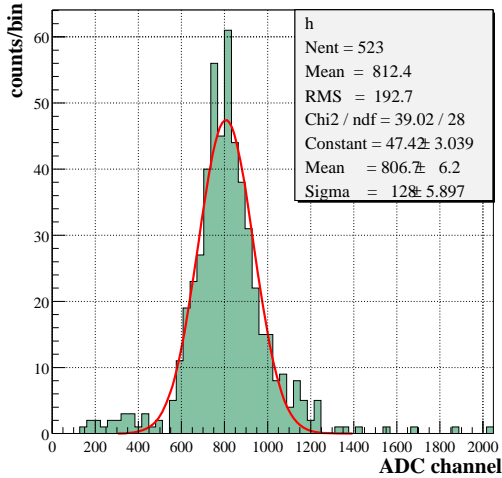


Figure 3: The cosmic muon signal detected by a Pb/SCIFI module. The average energy deposit of penetrating cosmic muons is about 12 MeV.

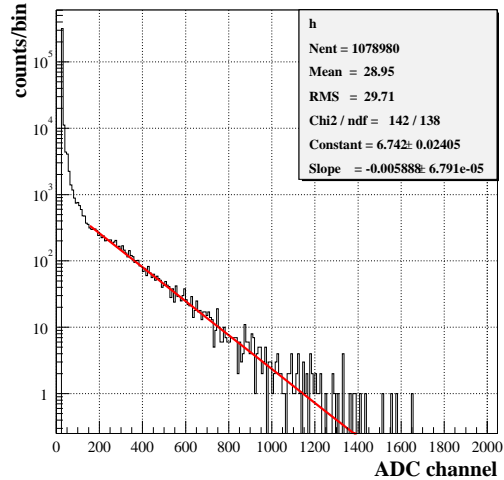


Figure 4: A typical raw ADC spectrum. The slope parameter of an exponential function is used for relative energy calibration.

cosmic muons passing through a module is about 12 MeV and this energy deposit corresponds to the incident photon energy of 200 MeV. High voltage values were set so that the dynamic range of ADC was equal to the photon energy of 2 GeV.

Then a photon beam was employed for energy calibration. As the statistics were not good enough to calibrate all the modules by using  $\pi^0$  events, the first relative calibration of modules was performed assuming azimuthal symmetry around the beam axis. An exponential function was fitted to each raw ADC spectrum (Fig. 4), separately. This resulted in a relative calibration for all modules placed in the same  $\theta$  by adjusting the slope parameters. The second relative calibration was done afterwards using the  $\pi^0$  peak reconstructed from 2-cluster events taking place in the same  $\theta$  row. The positions of reconstructed peaks obtained in different rows were then scaled to each other. The energy of the cluster was taken to be the energy deposited in the central module of the cluster up to this stage. For absolute energy calibration the same procedure was repeated but

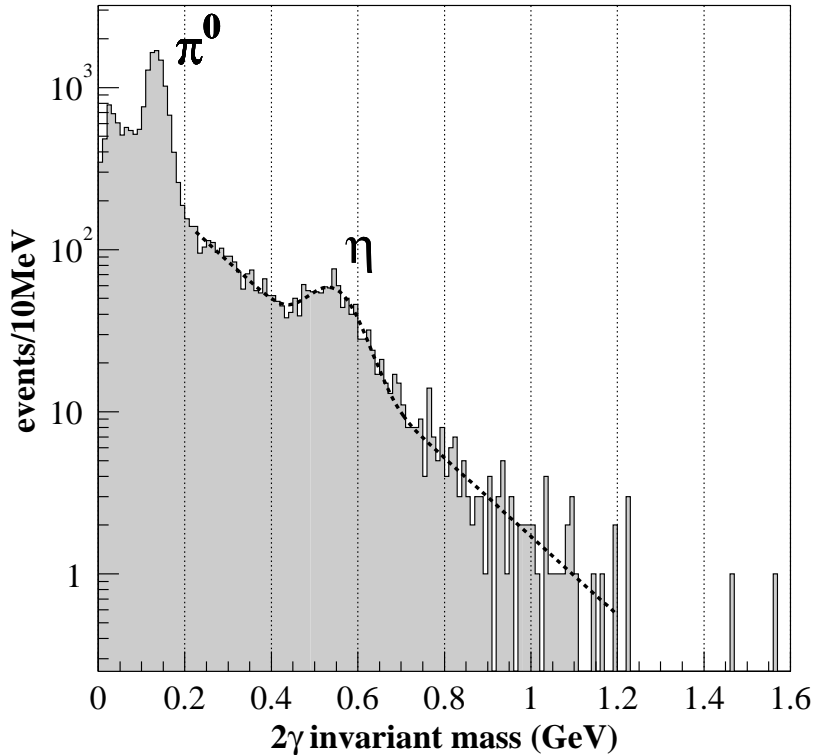


Figure 5: The reconstructed  $2\gamma$  invariant mass distribution after the energy calibration. The dotted curve is a fit to the data in the  $\eta$  mass region with a Gaussian function and an exponential background.

with summed energy of the clusters. Absolute energy calibration was made using the well-known  $\pi^0$  mass in the reconstructed  $2\gamma$  spectrum.

Fig. 5 shows the reconstructed  $2\gamma$  invariant mass distribution after the energy calibration. Here a center of gravity method was employed to obtain better localization of the  $\gamma$  clusters. One can see in the figure a calibrated  $\pi^0$  peak and a pronounced  $\eta$  bump around 550 MeV. The reconstructed  $\pi^0$  mass resolution is 19 MeV, corresponding to the relative resolution of 14%. The reconstructed  $\eta$  mass is  $543 \pm 5$  MeV and the mass resolution for the  $\eta$  is 10% for the moment. This shows that the energy calibration performed using  $\pi^0$  events works well for higher invariant masses. These values are very much preliminary. And we expect the resolutions will be improved in an advanced off-line analysis.

### 2.3.2 Clustering Algorithm

A clustering algorithm for obtaining correct photon hits has been developed based on the following strategy:

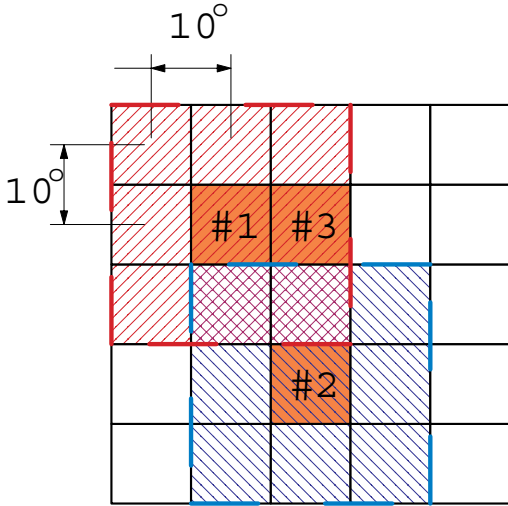


Figure 6: An illustration of a typical 2-cluster event. Three modules labelled #1,2,3 have energy deposit above  $E_{cut}$ . The numbering is such that  $E_1 > E_2 > E_3$ . The algorithm decides that #1 module with larger energy deposit is the central module of one cluster. Also the #2 module separated from the other two is considered to be the central module of the second cluster.

1. Modules whose signal exceeds a certain threshold  $E_{cut}$  are picked out from all modules. The sensitivity of the clustering algorithm varies with this  $E_{cut}$ . Reducing the threshold makes it more sensitive, but it also results in more complex hit pattern.
2. The algorithm judges whether those modules should be merged or separated by comparing a map which was prepared by means of a Monte-Carlo simulation beforehand.
3. Then the algorithm decides the central module of a cluster by comparing the magnitude of the deposited energy.
4. Finally this algorithm puts central and peripheral eight modules together and regards these as a one-cluster event. If there are shared modules, the deposited energy in the modules is simply divided into the number of the sharing clusters.

Fig. 6 shows an illustration of an example of the 2-cluster event.

## 2.4 Results of the Test Experiment

We had a chance to test the backward  $\gamma$ -detector with a linearly polarized LEPS beam. The targets used in the test experiment were  $C$ ,  $Cu$ , and  $W$  with a thickness of about 0.2 radiation lengths for all of them. In addition to that the  $CH_2$  target of the thickness of about 0.1 radiation lengths was also used.

Requiring the tagger signal, the event trigger signal was issued when at least one signal exceeded a threshold in the  $\gamma$ -detector modules placed within the region of  $40^\circ < \theta < 90^\circ$ . In the case of the carbon target, the trigger rate was about 300 cps at the beam intensity

of about  $5 \times 10^5$  photons/s which was measured by the tagger covering the energy of the tagged photons greater than 1.5 GeV. The background trigger rate without the target was about 160 cps. These background trigger events are due to the photons coming from the upper stream. And we can reduce the backgrounds by installing some photon-veto counters of lead glass just in front of the target.

We regarded it as a  $\pi^0$  event if the requirement  $|m_{\gamma\gamma} - m_{\pi^0}| < 3\sigma_E$  is satisfied. Here  $\sigma_E$  is the detector resolution at the pion mass region and  $\sigma_E \simeq 19$  MeV for the moment. The threshold  $\gamma$  energy is set to be 40 MeV in the present off-line analysis. There are

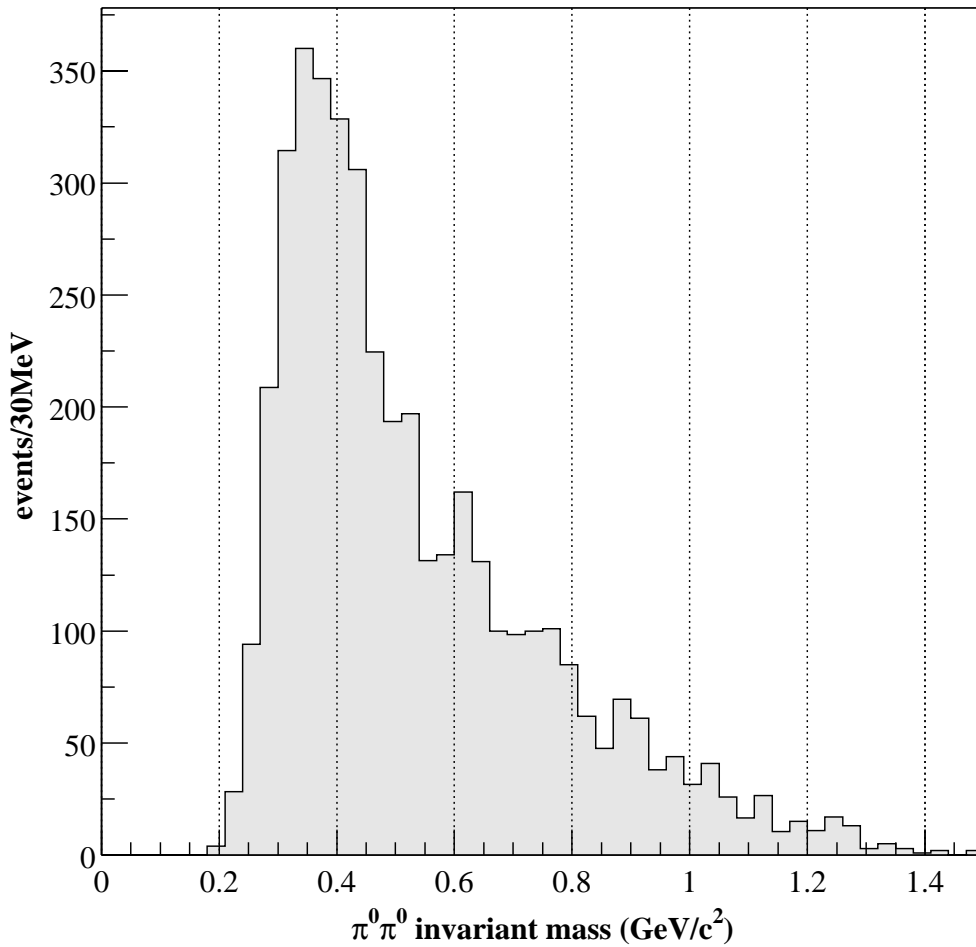


Figure 7: A preliminary  $\pi^0\pi^0$  mass spectrum in the  $\gamma C \rightarrow \pi^0\pi^0 X$  reaction for the incident photon energy of  $1.5 \leq E_\gamma \leq 2.4$  GeV. The acceptance correction is not made.

three different sets of combinations of two  $\gamma$ 's among four  $\gamma$  clusters in the process of reconstructing a  $\pi^0\pi^0$  event. By applying the criterion for the selection of a single  $\pi^0$ ,

described above, to all the combinations of the 4  $\gamma$ 's, we were able to reconstruct a  $\pi^0\pi^0$  event. The overall mass resolution of  $m_{\pi^0\pi^0}$  is evaluated to be about 30 MeV near the  $2\pi$  threshold. (The energy resolution of the incident photon beam was measured previously to be  $(15 \pm 5)$  MeV.) Fig. 7 shows the  $\pi^0\pi^0$  mass spectrum obtained with the  $C$  target, without the acceptance correction. The incident photon energy  $E_\gamma$  ranges from 1.5 to 2.4 GeV. The data with the  $C$  target were accumulated for 12 hours. In this test experiment outgoing protons were not detected. Therefore the acceptance correction is

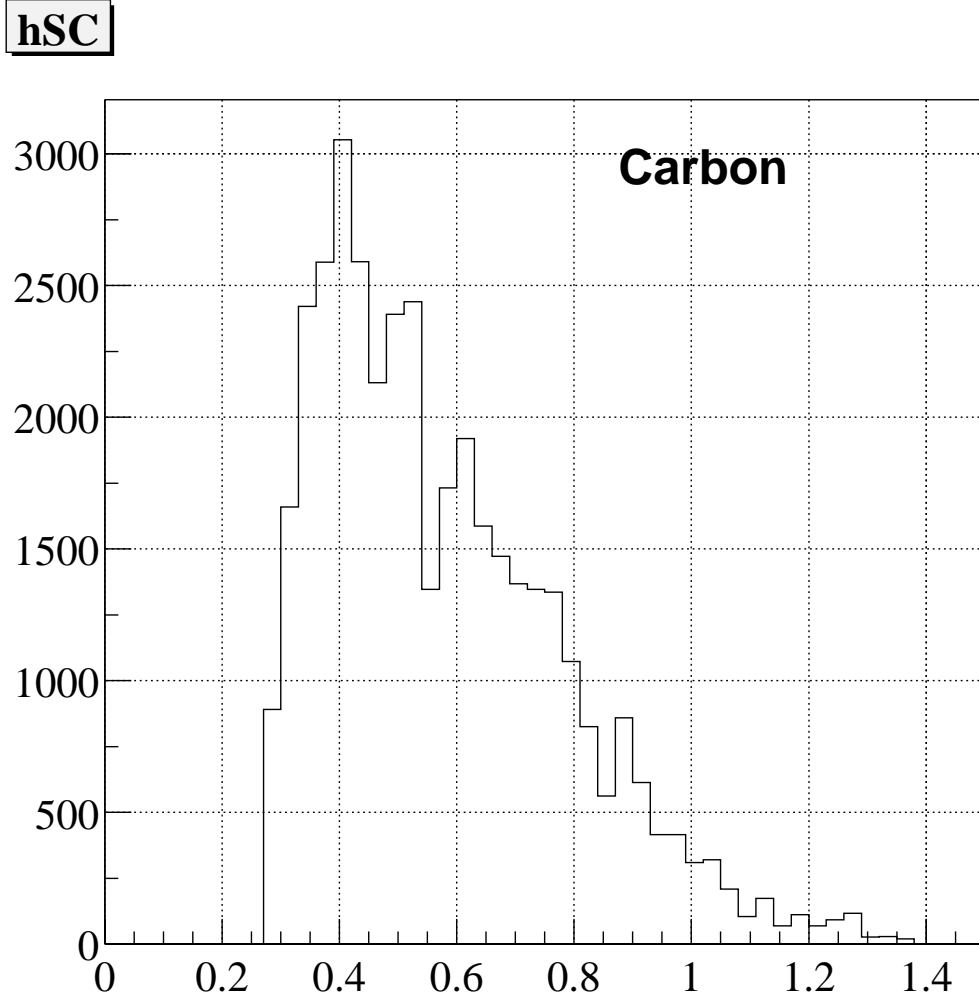


Figure 8: A preliminary  $\pi^0\pi^0$  mass spectrum in the  $\gamma C \rightarrow \pi^0\pi^0 X$  reaction for the incident photon energy of  $1.5 \leq E_\gamma \leq 2.4$  GeV. The acceptance is corrected under the assumption of a quasi-free nucleon target. The vertical axis has an arbitrary scale.

not straight forward. But the backward  $\gamma$ -detector has an acceptance only for the events at the high momentum-transfer region like  $|t| \geq 0.5$  GeV<sup>2</sup> in  $\pi^0\pi^0$  production. In such a high momentum-transfer region an incident photon interacts with a nucleon in the target nucleus rather than with the nucleus since the wave length of the transfer momentum is

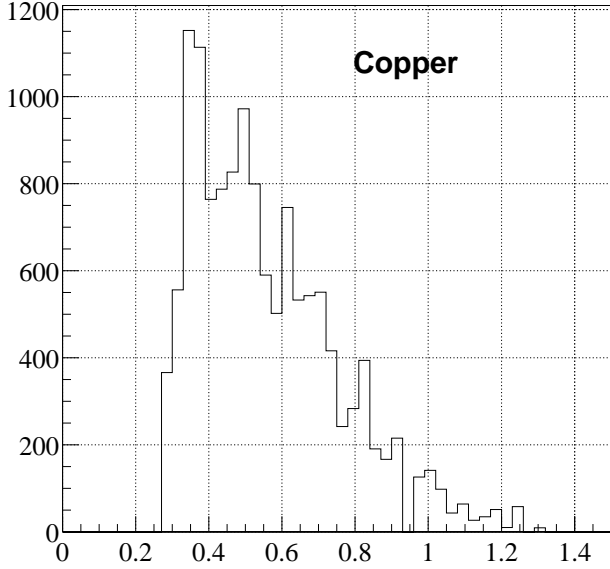


Figure 9: A preliminary  $\pi^0\pi^0$  mass spectrum in the  $\gamma Cu \rightarrow \pi^0\pi^0 X$  reaction for the incident photon energy of  $1.5 \leq E_\gamma \leq 2.4$  GeV. The acceptance is corrected under the assumption of a quasi-free nucleon target. The vertical axis has an arbitrary scale.

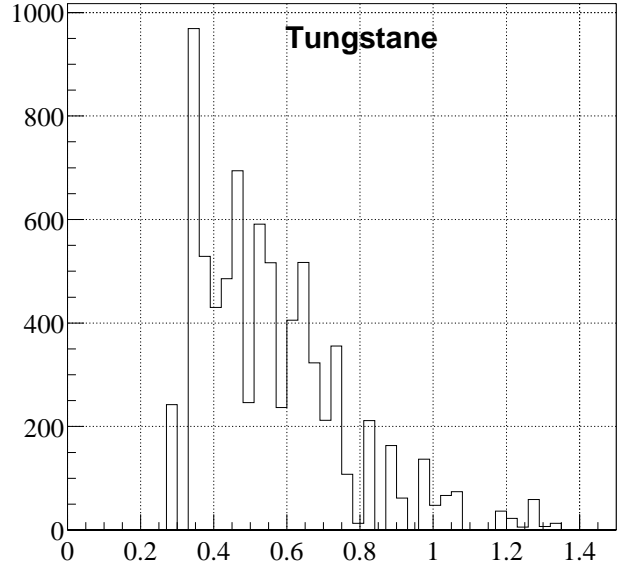


Figure 10: A preliminary  $\pi^0\pi^0$  mass spectrum in the  $\gamma W \rightarrow \pi^0\pi^0 X$  reaction for the incident photon energy of  $1.5 \leq E_\gamma \leq 2.4$  GeV. The acceptance is corrected under the assumption of a quasi-free nucleon target. The vertical axis has an arbitrary scale.

less than 1.8 fm. Then we made an acceptance correction for the data, provided a quasi-free nucleon target in the carbon, to obtain a preliminary result shown in Fig. 8. We have similar results with  $Cu$  and  $W$  targets as shown in Figs. 9-10 although the statistics are not good enough.

All these data shown here are for inclusive processes and very much preliminary. It is hard to say something definite about physics concerning the present data for the moment because the experimental conditions are rather vague. The outgoing protons have to be identified and the incident photons have to be separated into small energy bins. However we got important informations on the event rate of  $\pi^0\pi^0$  and on the different types of background, which had never been known before.

One more information obtained in the test experiment is about the measurement of the asymmetry parameter  $\Sigma$  in  $\pi^0\pi^0$  photoproduction. Fig. 11 shows the asymmetries of  $\phi$  distribution in the process  $\gamma C \rightarrow \pi^0\pi^0 X$  for different mass regions. The function  $P\Sigma \cos 2\phi$  was fitted to the data. And the obtained average asymmetry  $P\bar{\Sigma}$  is  $0.025 \pm 0.026$  for the mass region of  $m_{\pi^0\pi^0} < 500$  MeV and that for the mass  $m_{\pi^0\pi^0} > 500$  MeV measures  $-0.043 \pm 0.032$ . Here  $P$  is the beam polarization and the average asymmetry  $\bar{\Sigma}$  means that the data are summed up for all the available  $\theta$ . If we have much more statistics, we can investigate the  $\theta$  distribution of the asymmetry  $\Sigma(\theta)$  which usually has a shape and is

therefore locally larger than the average asymmetry  $\bar{\Sigma}$ . The events corresponding to the different beam energies are integrated in the present off-line analysis from 1.5 to 2.4 GeV to get more statistics. This gives rise to dilution of the average beam polarization since the polarization of the LEPS beam is energy dependent. And hence we have very small asymmetries. In the proposed experiment we will have good statistics enough to get the

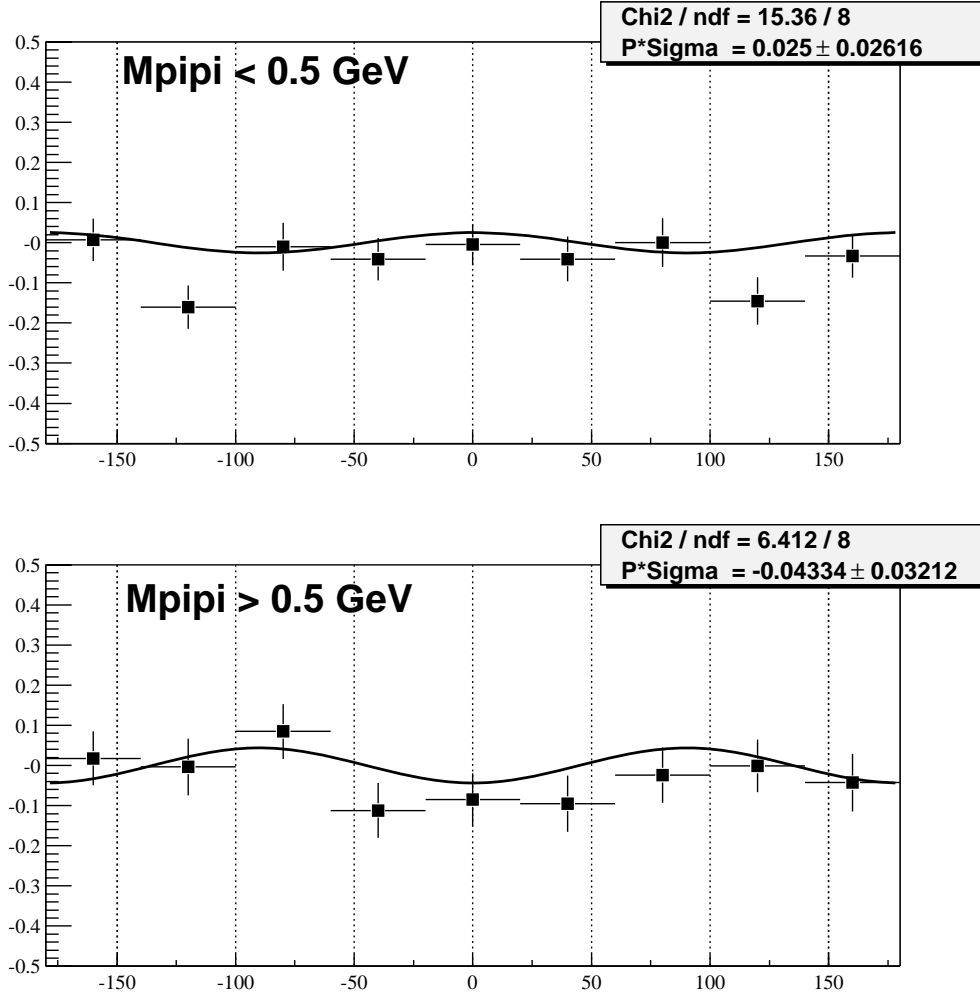


Figure 11: The average  $\phi$  distribution in the process  $\gamma C \rightarrow \pi^0 \pi^0 X$ . The upper part shows the  $\phi$  distribution for  $m_{\pi^0 \pi^0} < 500$  MeV and the lower part corresponds to that for  $m_{\pi^0 \pi^0} > 500$  MeV. The solid lines show the results obtained by fitting the function  $P\Sigma \cos 2\phi$  to the data.

$\Sigma(\theta, E_\gamma)$  distributions for the mass region of  $m_{\pi^0 \pi^0} < 300$  MeV.

## 2.5 Data Statistics

This is the estimations of the data statistics to be expected in the proposed experiment. All the estimations are based on the data obtained in the test experiment with the fol-



lowing conditions.

1. The intensity of the LEPS beam is assumed to be  $1 \times 10^6$  photons/s.
2. The target thickness is 0.2 radiation length.

### 2.5.1 Expected Yield

We evaluated the number of events for  $\pi^0\pi^0$  photoproduction as a function of mass  $m_{\pi^0\pi^0}$ , the momentum of the  $\sigma$  ( $2\pi^0$  system) and the momentum transfer. Here we show the results of our estimation for them in the case of the Carbon target. We assume 7 days for running with the  $C$  target. The total number of events for  $\pi^0\pi^0$  production is presented in Table 1 as a function of the momentum transfer  $t$ . Then the dependence of the yield

Table 1: Number of  $\pi^0\pi^0$  events with the  $C$  target.

$ t (\text{GeV}/c)^2$	0.5-1.0	1.0-1.5	1.5-2.0	2.0-2.5	2.5-3.0
# of events	16811	16811	8027	2549	646

on the mass of  $\pi^0\pi^0$  is shown in Table 2. The number of events for the  $\pi^0\pi^0$  system of  $0.2 < m_{\pi^0\pi^0} < 0.4$  GeV is presented in Table 3 for the momentum-transfer region of  $0.5 < |t| < 1.0$  GeV<sup>2</sup> as a function of the momentum of the system.

Table 2: Number of  $\pi^0\pi^0$  events with the  $C$  target as a function of  $m_{\pi^0\pi^0}$ .

$m_{\pi^0\pi^0}$ (GeV)	0.2-0.4	0.4-0.6	0.6-0.8	0.8-1.0	1.0-1.2	1.2-1.4
$0.5 <  t  < 1.0$	8930	4709	1659	988	390	97
$1.0 <  t  < 1.5$	5063	6319	3098	1403	719	183
$1.5 <  t  < 2.0$	1866	2476	1952	1073	463	183
$2.0 <  t  < 2.5$	414	671	622	463	305	73

Table 3: Number of  $\pi^0\pi^0$  events with the  $C$  target as a function of the momentum.

momentum (GeV/c)	0-0.2	0.2-0.4	0.4-0.6	0.6-0.8	0.8-1.0
	854	4916	2610	439	97

For the mass of  $0.2 < m_{\pi^0\pi^0} < 0.4$  GeV and  
for the momentum transfer  $0.5 < |t| < 1.0$  GeV<sup>2</sup>.

Table 4: Number of  $\pi^0\pi^0$  events with the  $C$  target as a function of  $m_{\pi^0\pi^0}$  and  $\theta$ .

$m_{\pi^0\pi^0}$ (GeV)	0.2-0.4	0.4-0.6	0.6-0.8	0.8-1.0	1.0-1.2	1.2-1.4
$80^\circ < \theta < 90^\circ$	512	475	244	122	36	24
$90^\circ < \theta < 100^\circ$	1891	1500	756	414	97	12
$100^\circ < \theta < 110^\circ$	4245	2842	1183	573	183	24
$110^\circ < \theta < 120^\circ$	4440	3574	1512	585	244	73
$120^\circ < \theta < 130^\circ$	3306	2769	1427	768	305	61
$130^\circ < \theta < 140^\circ$	585	658	549	329	146	48
$140^\circ < \theta < 150^\circ$	646	829	707	475	317	61
$150^\circ < \theta < 160^\circ$	195	402	305	134	195	109

For the asymmetry measurement the mass distribution of the events is obtained for every  $10^\circ$  in the CM angle assuming the quasi-free  $\gamma p \rightarrow \pi^0\pi^0 p$  process. The estimated yield for the mass of the  $\pi^0\pi^0$  system is shown in Table 4. This result indicates that the asymmetry  $\Sigma(\theta)$  can be measurable for each mass bin of 200 MeV. The beam energy is, however, integrated from 1.5 to 2.4 GeV here and the estimation is based on the result of the inclusive reaction. Therefore the number of events may be 1 order smaller than that shown in the table to get the detail sets of the data like  $\Sigma(E_\gamma, m_{\pi^0\pi^0}, \theta)$ . It is possible to improve the statistics by increasing the beam intensity up to  $5 \times 10^6$  photons/s, which is quite feasible at the LEPS beam line. At the same time we can reduce the trigger rate by adding the signal of charge-veto counters placed inside the  $\gamma$  detector to the trigger logic.

### 2.5.2 Target Empty Run

We have observed background triggers without targets in the present set-up. It is conceivable that those triggers are caused by the beam halo hitting the duct and the shielding blocks placed upstream the detectors. We are planning to reduce them by installing  $\gamma$ -veto counters of lead glass just in front of the target. But here we estimate the run time for the empty target by making use of the result of the test experiment. Table 5 shows

Table 5: Running time estimation.

target	target run	empty run
$C$	7 days	2.8 days
$Cu$	7 days	4.1 days
$W$	7 days	5.4 days

the running time with a nuclear target and that with the empty target under the same condition of the test experiment. Here the running time for the target empty run is estimated so as to make the statistical error of the background-subtracted data minimum. We expect that the situation will be improved by employing  $\gamma$ -veto counters. Therefore we request 30 days in total for data acquisition.

### 3 Conclusion and Requests

It is very important in QCD and hence in hadron physics to find precursors to the chiral transition. The inside of the nucleus is one of the good candidates where partial restoration of chiral symmetry takes place and therefore some kinds of precursors may appear. The photon beam is useful in producing mesons effectively inside the nucleus. The  $\sigma$  meson in the nucleus is the most appropriate to be investigated in this regard since it corresponds to the quantum fluctuation of the chiral order parameter. There was a long standing puzzle about the existence of the  $\sigma$  meson. Nowadays the riddle of the  $\sigma$  is recast in a way that tries to find the position of the pole of the  $\sigma$  in the complex energy plane.

We try to find a precursor phenomenon to the chiral transition by measuring  $\pi^0\pi^0$  events in the  $\gamma A \rightarrow \pi^0\pi^0 pX$  process in conjunction with the behavior of the  $\sigma$  in nuclei. The asymmetry observable  $\Sigma(\theta)$  for this process will also be measured to see any clue to the precursor in this spin observable. These measurements with nuclear targets will be made for the first time in the world in the multi-GeV energy region.

The lineally polarized LEPS beam is ready with a sufficient intensity and excellent polarization. The main detector for the experiment is ready. The manpower is ready to go. In summary we request 30 days of effective data taking, preceded by 2 days for tuning and calibration. We require the beam intensity of  $\geq 2 \times 10^6$  photons/s.

### References

- 1) T. Hatsuda, T. Kunihiro and H. Shimizu, Phys. Rev. Lett. 82 (1999) 2840.
- 2) D.W. Hertzog *et al.*, Nucl. Instr. Meth. A294 (1990) 446;  
D. Babusci *et al.*, Nucl. Instr. Meth. A332(1993) 444.